공학석사 학위논문

Construction of High-resolution Patterns of Solution-processed Organic Light-emitting Diodes Using Surface Modified Banks by Wettability

격벽 구조의 표면 젖음성 조절을 통한 용액공정 기반의 유기발광 다이오드의 고해상도 패터닝에 관한 연구

2017 년 2 월

서울대학교 대학원

공과대학 전기·정보공학부

김 휘

Construction of High-resolution Patterns of Solution-processed Organic Light-emitting Diodes Using Surface Modified Banks by Wettability

지도교수 이 신 두

이 논문을 공학석사 학위논문으로 제출함

2017 년 2 월

서울대학교 대학원

공과대학 전기·정보공학부

김 휘

김휘의 공학석사 학위논문을 인준함

2017 년 2 월

위 원 장 이 창 희 (인)

부위원장 이 신 두 (인)

위 원 홍 용 택 (인)

Abstract

In the field of flat-panel displays, solution-processed organic light-emitting diodes (S-OLEDs) have attracted considerable attention due to the applicability of low-cost, low-temperature, and large-area processes. For manufacturing S-OLEDs, much effort has been made toward the development of simple and reliable methods of patterning individual elements of the S-OLEDs. One of widely used techniques for patterning a solution is based on insulating banks to define solution patterns without any detrimental effect on the device performances. However, it suffers intrinsically from the pattern resolution as well as the pattern fidelity since the formation of high-density insulating banks on a substrate significantly deteriorates the wetting nature of a solution. Thus, the delicate control of the surface wettability of a bank-structured substrate (BS) is inevitably required for achieving the high level of the pattern resolution and fidelity of the solution.

This study presents a viable method of producing high-resolution patterns for pixels in the S-OLED with the aid of ultraviolet ozone (UVO)

treatment on the BS. The insulating banks were first prepared through the injection of photo-curable polymer (NOA 74) into the channels between a pre-patterned polydimethylsiloxane (PDMS) stamp and an indium-tin-oxide (ITO)-coated glass substrate by capillary action and subsequently cured under the ultraviolet (UV) light. The modification of the surface wettability of the BS was carried out by the UVO treatment as a function of time. From the results for the contact angles of the water, the surface of the BS was found to be greatly modified from hydrophobic surface to hydrophilic surface with increasing the treatment time. Using the insulating banks of 5 μm and 10 μm in line width and space, the corresponding S-OLEDs patterns were fabricated with high resolution. Also, S-OLED was fabricated with identical fabrication method on the flexible substrate which is one of the features of next generation display. This wettability-controlled patterning approach will provide a useful platform to construct next generation displays from solutions in the manner of high resolution over large area and low cost.

Keywords: Solution-processed organic light-emitting diode, Contact angles, soft-lithography, Patterning OLED pixel, Flexible display

Student Number: 2015-20916

TABLE OF CONTENTS

LIST OF FIGURES

1. Introduction

1.1. Organic light-emitting diodes

Organic light-emitting didoes (OLEDs) have attracted much attention due to their superior characteristics such as viewing angles, high contrast ratio, fast response time and low power consumption. The OLED flat-panel displays also have potentials for applications in flexible display. Since C. W. Tang in Eastman Kodak Company first reported the organic electroluminescent diodes in 1987 [1], performances of the OLED devices have showed dramatic progress by many researchers. Electro-phosphorescent organic light-emitting devices with an internal quantum efficiency of nearly 100% have been demonstrated [2-3] and long device lifetimes of the red, green and blue diodes were reported. Recently, the OLED displays are regarded to have great potentials for next generation displays.

The OLED devices, however, still have many obstacles to achieve competitive performances compared with liquid crystal display (LCDs) and

other types of flat panel displays (FPDs). In spite of the high internal quantum efficiency of the devices, the external quantum efficiency for a conventional OLED device is relatively low. Because of the high refractive index of organic materials and the optical confinement and internal reflection that results, the light out-coupling efficiency for a conventional OLED device is limited to about 20 % [4-5].

Furthermore, the conventional bottom-emitting OLED displays need additional components to achieve the high contrast ratio in ambient conditions. Although the OLEDs emit little light in their off-states, so that the contrast ratio of the device can be high enough in dark environments, because of the high reflectance of the back electrode, which is typically a metallic cathode, the contrast ratio of the devices were significantly reduced in bright environments. There were many strategies to reduce reflectance and ensure the high contrast ratio in the ambient conditions, but they commonly have drawbacks such as high costs and increased thickness of the devices [6-7].

A typical bottom-emitting OLED has a transparent anode, a metallic cathode and organic materials between them. The first electroluminescent

diode reported by C. W. Tang had a single organic layer consists of 8-hydroxyquinoline aluminum (Alq_3) as an emitting layer [1]. After a multi-layer structure was introduced [8], the OLEDs have increased their number of layers to improve the light-emitting efficiency of the diodes. The structure consists of the electron injection layer (EIL), the electron transport layer (ETL), the emitting layer (EML), the hole transport layer (HTL) and the hole injection layer (HIL) as shown in Fig 1.1 is widely used for the conventional OLED devices recently.

Organic materials are intrinsically non-conducting, however in the solid-state, electrons in a molecule which do not participate in the covalent bonding, form π-electrons. These electrons are delocalized and form polarons by coupling with lattices. The polarons in a certain molecule can move to other molecules through hoping transportations, so that the organic materials show semiconducting electrical properties.

By interactions between covalent electrons and orbital, the energy levels of bonding orbital and anti-bonding orbital differ. Consequently, the organic materials have highest occupied molecular orbital (HOMO) and lowest

unoccupied molecular orbital (LUMO), and the band-gap of the organic material can be defined similar to the in organic semiconductors.

In Fig. 1.3, an energy band diagram for the typical OLED consists of three organic layers, which are the HTL, the EML and the ETL, is illustrated. From an anode has high work functions, holes are injected into the HTL and electrons are injected into the ETL from a cathode has low work functions. The holes and electrons, finally injected to an emitting layer, forms excitons, which are the hole-electron pair have excited energy levels. These excitons release energy by recombination and some fraction of excitons emit energy in a form of photons.

The excitons are classified into the singlet and the triplet, which correspond to spins of the electrons and holes. An exciton without net spin form a singlet and a triplet have net spins. Since the electrons and the holes injected from the cathode and the anode have random spins, the ratio of the formation of the singlet and the triplet is 1 : 3 [9].

As a result, electro-fluorescent devices which use only singlets to emit light can have the internal quantum efficiency reach to maximum 25 %

theoretically. On the other hand, electro-phosphorescent devices which utilize triplets to emit photons can have the internal quantum efficiency reach to 100 % by energy transfers to dopant materials. In 1998, the Forrest's group reported the first electro-phosphorescent devices [2], and demonstrated the device with the internal quantum efficiency near 100 % in 2001 [3].

Moreover, solution-processed OLEDs have long been viewed as a potentially lower cost, higher efficiency method for producing OLED displays. Thermal evaporation process under high vacuum increases fabrication complexity and makes the utilization of the expensive OLED materials very low. Additionally, pixelation using evaporation masks would limit its scalability and resolution. The best way to improve the efficiency of the process and reduce the production cost is to use solution process for the fabrication of OLEDs. The fabrication methods based on solution process have advantages of manufacturing large-area, high-resolution full-color flat-panel displays. Additionally, its possibility applicable on the flexible substrate is the reason that S-OLEDs are viewed as a potential method for producing next generation display.

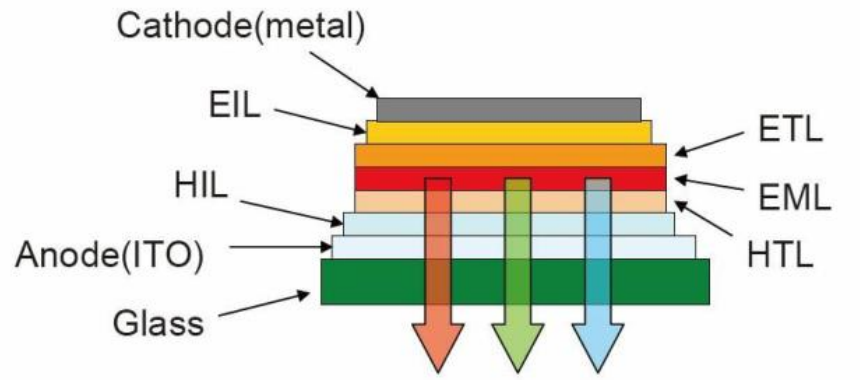

Fig. 1.1 Schematic of a typical bottom-emitting OLED device.

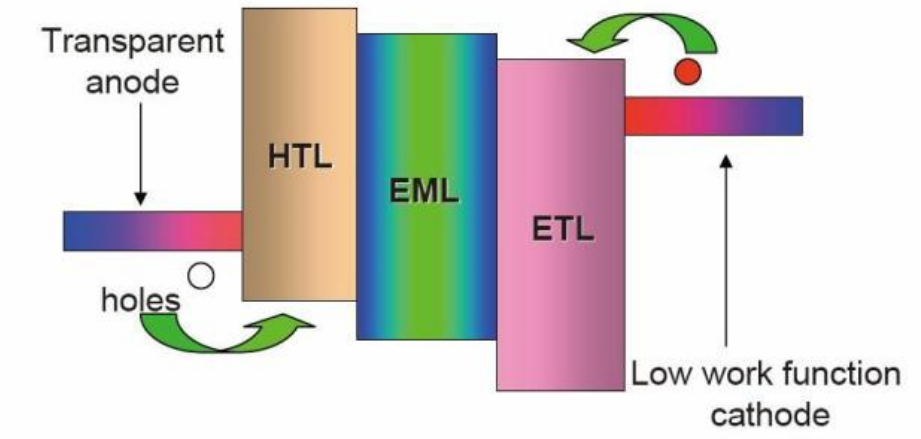

Fig. 1.2 Energy band diagram of an OLED with three organic layers.

1.2. Patterning Technologies of Pixels in OLEDs

In general, patterning technologies are crucial issues for fabricating the OLEDs especially for solution process. In OLEDs, each pixel consisted of three OLED subpixels of the primary colors and must be confined to the selective region for emitting and driving each pixel. For small displays like microdisplay, high resolution with high pixel density density patterning technique is needed because of a short viewing distance.

In order to create the required pixel patterns for flat panel display, two different technologies have been employed in the manufacture of OLED displays, that is conventional vapor deposition and solution processing.

Shadow Mask Patterning with thermal deposition

Thermal sublimation in vacuum is the most common means for depositing small molecular organic thin films. This process involves the heating of the source material in a vacuum chamber, with the substrate located several centimeters distant, usually placed above the source. Thermal evaporation is

widely used in the processing of inorganic semiconductor devices because of the precision with which layer thicknesses can be controlled (typically to within 0.5 nm), and the relative simplicity of the process. One particular advantage of thermal evaporation is its ability to grow an unlimited number of layers, each optimized for a different function, to complete the device structure. This flexibility in device design is an inherent feature of dry processing that is, the several material layers that are deposited to form a device structure do not physically interact because there is no solvent that might transport material and chemically attack the pre-deposited film. This compatibility between layers provides for enormous flexibility in choosing materials and structures to be used in complex, modern electronic devices. In thermal evaporation, various patterns can be easily produced by adding a shadow mask, which is usually a thin metal film with holes of desired patterns, between a source material and a substrate in a chamber. However, blurs and errors can be generated, as the size of the substrate increases or the features become smaller, by the sagging of thin metal mask due to the gravitational force, resulting in the limitation of pattern resolution over the large-area.

Ink-jet Printing

One emerging patterning strategy for solution-processed OLEDs is ink-jet printing. Patterns can be generated by ejecting a droplet of the solvated polymer from a micrometer-scale nozzle from a modified ink-jet printer and subsequently driving off the solvents from the droplet landed at the substrate. The ink-jet printing method enables to locally produce the parallel patterns of different classes of materials, while the entire substrate is coated with only a single material by the general solution processes including ’spin-on’ or ‘spray-on’, and is demonstrated to fabricate full color organic light emitting diode displays. However, it is still difficult to produce precise patterns through ink-jet printing since the pattern dimension is usually determined by the range where the polymer ink spreads out. Some kinds of preprocessing, therefore, are additionally required such as a fabrication of well structures to physically block the spread of polymer ink. Such structures might limit the freedom of designing device structures, and thus various surface treatments using plasma or UV are recently attracted much attention to locally control the surface wettability.

Spin-coating

Spin coating is a procedure used to deposit uniform thin films to flat substrates. Usually a small amount of coating material is applied on the center of the substrate, which is either spinning at low speed or not spinning at all. The substrate then rotated at high speed in order to spread the coating material by centrifugal force. A machine used for spin coating is called a spin coater, or simply spinner. The advantage of spin coating is its ability to easily and quickly form very homogeneous film over large areas. It is used in the microelectronics and industry with many materials from photoresist to nanomaterials. However, the spin coating is an inherently single substrate process and therefore relatively low throughput compared to roll-to-roll processes. The fast drying times can also lead to lower performance for some particular nanotechnologies which require time to self-assemble and crystallize.

Roll-to-roll Printing

Roll-to-roll printing known as R2R is the process of forming film of electronic devices of a roll of flexible substrate and metal foil as it transferred between two moving rolls of material. R2R printing has advantage of high throughput and low cost compared to conventional manufacturing which is slower and high cost. R2R processing can be applied in a variety of manufacturing field such as flexible and large-scale microelectronics, plastic solar cell panel, metal foil, and fibers. R2R processing is still in development, if semiconductor and solar cells could be fabricated by this technology, it can be a potential system to produce numerous electronics with low cost over large areas. However, initial capital costs of R2R systems can be high to set up all of systems.

1.3. Photolithography and Softlithography

Photolithography

Photolithographic techniques have been widely used in the inorganic semiconductor industry, which have the capability of high resolution and high throughput as well as the availability of well-established equipment and expertise. Patterning of thin films based on the photolithographic processes can be generally divided into two different methods, one of which is ‘additive’ and the other are ‘subtractive’. In the ’additive’ method, the target film is deposited onto the preformed photoresist (PR) patterns and subsequently lifted-off by removing the PR simultaneously with the residual thin films on it, leaving only the desired thin film patterns on a substrate. On the contrary, the etching process is used in the ‘subtractive’ method.

The PR is first patterned on a pre-deposited thin film to be used as a ‘etching mask’. The following etching process to erase the thin film exposed to the solvent completes the pattern generation on a substrate. Such two types of photolithographic patterning processes commonly have not been used in

the fabrication of organic electronic devices mainly due to the chemical incompatibility. Organic solvents or other agents used in the photolithography might chemically attack or dissolve the pre-deposited organic films.

Soft lithography

Microcontact printing

Microcontact printing (μCP) is one of the soft lithography that uses the relief patterns on a master PDMS stamp to form patterns of self-assembled monolayers of ink on the surface of a substrate through conformal contact. Its applications are wide ranging including microelectronics, surface chemistry and cell biology. The μCP printing can be used in several different ways. The pattern generated by the printing can serve as an etch mask or it can become a patterned active area or it can define the electrodes. It can also be used to create a medium by which selective deposition is possible. Moreover, the μCP printing has been used to advance the understanding of how cells interact with substrates. This technique has helped improve the study of cell patterning that

was not possible with traditional cell culture techniques.

Imprint lithography

Imprint lithography [10] can also be used for the patterning for the fabrication of organic electronic or electro-optic devices such as OLED. One distinct advantage of imprint lithography is its simplicity. The single greatest cost associated with device fabrication is the optical lithography tool used to print the circuit patterns. Also, imprint lithography is inherently a three-dimensional patterning process. Imprint molds can be fabricated with multiple layers of topography stacked vertically. Resulting imprints replicate both layers with a single imprint step, which allows device manufactures to reduce device fabrication costs and improve product throughput. Moreover, the imprint material does not need to be finely tuned for high resolution and sensitivity. A broader range of materials with varying properties are available for use with imprint lithography. The increased material variability gives chemists the freedom to design new functional materials rather than sacrificial etch resistant polymers. A functional material may be imprinted directly to

form a layer in a chip with no need for pattern transfer into underlying materials. The successful implementation of a functional imprint material would result in significant cost reductions and increased throughput by eliminating many difficult chip fabrication processing steps.

Transfer patterning

Transfer patterning [11] can be used not only for the transfer of one layer but also for multiple layers. Therefore, the method can be used to realize entire device transfer for patterns in the vicinity. In one example the multi-layer structure of the organic light emitting diode including the cathode is transferred onto a patterned ITO anode on a glass substrate. Fluorinated ethylene propylene is, often, first deposited on a mold to reduce the work of adhesion at the mold interface, followed by sequential depositions of the aluminum cathode and organic multilayer stacks. Device transfer is accomplished by pressing the coated mold onto the substrate at a pressure ranging from 1 to 5 MPa at 50 ◦C for 5 min. After cooling to room temperature, the mold is simply removed, thereby, transferring the device

structure on the protruding parts of the mold to the substrate. After the 1st pixel is fabricated, the same procedure can be followed for aligning and transferring 2nd and 3rd pixels for RGB pixelation in organic light emitting diodes. The performance of the devices thus fabricated is equivalent to those formed in the conventional way.

Micromolding in capillaries

Micromolding in capillaries (MIMIC) [12] is a simple and convenient method to fabricate micro/nano structures of polymers and ceramics. It is based on the spontaneous injection of capillaries formed between substrate and elastomer (PDMS) with conformal contact. The injection material may be a liquid prepolymer, a solution, or precursor of the materials. After filling an organic or inorganic material in the channels, the materials in the fluid are crystallized and cured, and then the elastomeric PDMS is removed. Finally, the pattern of materials remains on the substrate. This technique is also used in the microelectronics such as OLED to pattern and define pixels. It can be used for advantages of low-cost and large-area fabrication.

1.4. Insulating Bank Structure for Pixel Patterning

The pixels in a practical OLED display are commonly defined based on the insulating bank structure. It is simple and reliable method without detrimental effects on OLED device performance. Especially for solution process fabrication without fine metal mask, insulating banks are essential structure for pattering pixels in the OLED display. As shown Fig. 1.3, various reports using insulating banks structure have been published in a solution process fabrication such as bar coating and ink-jet printing [13-16].

In general, the methods of fabricating this insulating bank structure essential for S-OLEDs can be divided in two categories, photolithography and softlithography as mentioned before. In recent years, numerous studies have attempted to confine OLED pixels using insulating bank structure by photolithography [13-18]. Although this approach have advantages of being conventional semiconductor processing, it involves various kinds of problems that it is a complex and high-cost process and has a degradation of performance due to photo resist and etching gas. Because of these

disadvantages of photolithographic processing, softlithographic processing has recently been studied. As shown Fig. 1.4, soft lithographic methods such as micro-molding in capillaries and micro replica molding have been proposed for confining OLED pixels [19]. It is a simple and low-cost process, however it has a problem that has large pattern size (~100 μm) due to its surface roughness. For this reason, more detailed study is necessary for high-resolution patterns using insulating structure bank by soft lithography. In this paper, we present the delicate control of the surface of insulating bank and viable method of patterning OLED pixels.

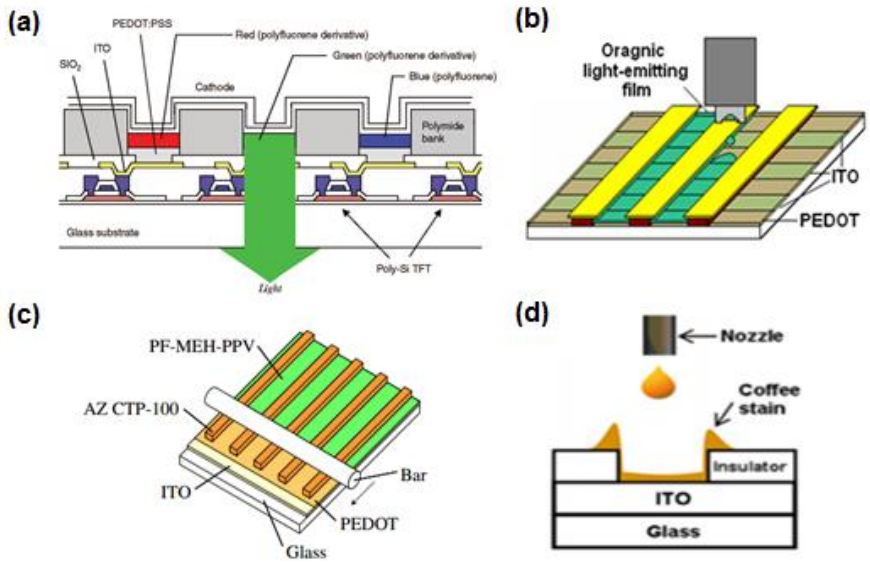

Fig. 1.3 S-OLEDs based on insulating bank structure.

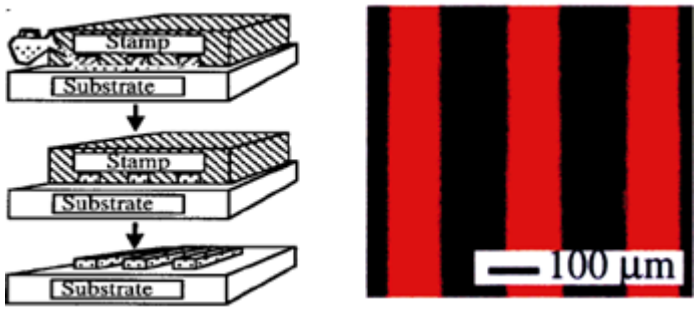

Fig. 1.4 S-OLED based on insulating bank structure by soft lithography.

1.5. Outline of thesis

This thesis consists of five chapters from **Introduction** to **Conclusion**. In **Chapter 1**, a general overview of the OLED and its working principles. The brief description of the patterning technologies of pixels in OLEDs and the insulating structure by photolithography and softlithography is also introduced in this chapter. **Chapter 2** provides the theoretical background for understanding contact angle and wettability of a solution on the bank-structured substrate. The surface modification by UV-Ozone treatment is also discussed in this chapter. **Chapter 3** presents the experimental procedures of this research. The fabrication process through MIMIC of softlithography and the characterization of the fabricated device are covered as well in this chater. In **Chapter 4**, the results of the experiments are presented and discussed. Finally, in **Chapter 5**, some concluding remarks are made.

2. Theoretical Background

2.1. Contact Angle of Bank-structured Substrate

Wettability has been described as a tendency of one fluid to spread or adhere to a solid surface in the presence of another immiscible fluid [20]. Wettability affects many aspects in modern physical sciences. To name a few, these include manufacturing of photo films, detergents, paper products, cosmetics, painting, and spreading of contact lens on human eye are all related with.

The contact angle (θ_{CA}) is a common and useful measure of wettability in a quantitative means of evaluating the surface wetting (or dewetting) tendency [21]. The contact angle is the angle that consists of the solid surface and the tangent of the liquid-vapor interface at the three different phase junction, illustrated as in the schematic of Fig. 2.1. The contact angle is in the range of 0 ~ 180°, 0° for the so-called complete wetting and 180° for the perfect dewetting. If the contact angle ranges from approximately 75° to 115° as shown in Fig. 2.2, it is considered to belong to the intermediate wetting

range. In general, for the contact angle measured with de-ionized water, the surface is mentioned as hydrophilic for θ_{CA} < 90°, and hydrophobic for θ_{CA} > 90°, respectively. In details, when a liquid drop is in conformal contact with a perfectly smooth, homogeneous solid substrate, it has characteristic angles on the substrate in order to minimize the free energy of a specific thermodynamic system. First, the contact angle is related with the interfacial free energies for a specific solid/liquid system represented by the equation of,

$$\gamma_{LV} \cos \theta_{CA} = \gamma_{SV} - \gamma_{SL} \tag{2.1}$$

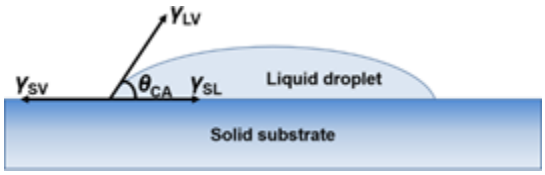

Fig. 2.1 Schematic illustration of contact angle of a drop on a solid surface.

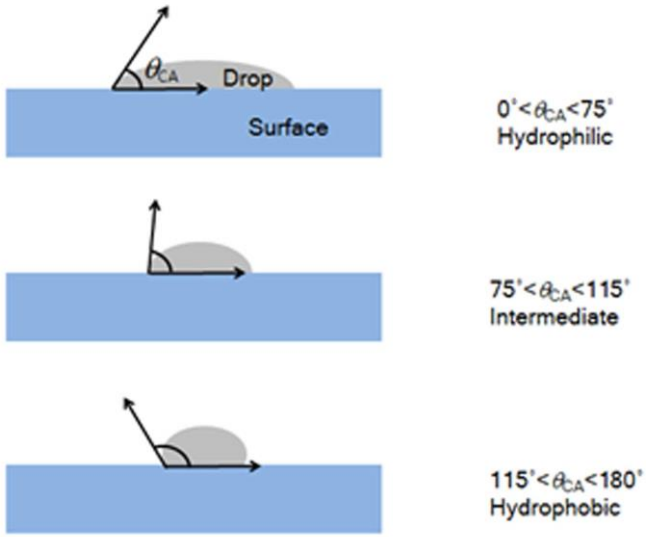

Fig. 2.2 Definition of wettability with contact angles.

where θ_{CA} is the contact angle, γ_{SV} is the solid-vapor interfacial free energy, γ_{SL} is the solid-liquid interfacial free energy, and γ_{LV} is the liquid vapor interfacial free energy. This equation is known as Young's equation [22]. Young's equation is widely used, but its simplicity requires additional understanding to be applied for specific systems. As explained, the contact angle measurement is very sensitive to the surface chemistry or physics since the interfacial free energies, γ_{SV} and γ_{SL}, are determined by the most outer part of the surface. The contact angle is hence very sensitive to the surface

contamination. Furthermore, both liquid drop and environmental immiscible liquid are important. It is because that the contact angle measurement is related to the physiochemical energy of the surface and the interfacial energies between the three different phases. In fact, the measured angle is not consistent always and varied within a certain range. This contact angle hysteresis results from the volume change of liquid drop and surface heterogeneity. Usually, the two angle limits, advancing angle and receding angle, remain relatively constant for a specific solid/liquid system. Advancing angle is measured when the liquid front just subsequent to move over a surface. On the other hand, receding angle is measured when the liquid front start to retract over the already wetted surface.

The actually measured constant angle is also affected by the surface roughness. The roughness-induced angle chage has been described by the Wenzel equation [23]

$$cos\,\theta_{CA} = rcos\theta \tag{2.2}$$

where θ_{CA} is the actually measured angle and θ is the equilibrium angle for perfectly flat surface, r is roughness ratio, namely the ratio of the true

surface area including the hill and valley and the apparent surface area. From the Wenzel equation, it suggests that in contact angle measurement, the surface roughness makes hydrophilic surface to appear more hydrophilic, and hydrophobic surface to appear more hydrophobic.

When dealing with a composite surface, not homogeneous surface, the Wenzel model is not sufficient. A more complex model is needed to how the apparent contact angle changes when various materials are involved. This heterogeneous surface is explained using the Cassie-Baxter equation [24]

$$cos\,\theta_{CA} = \sum xi\,cos\,\theta_i \qquad (2.3)$$

where θ_{CA} is the actually measured angle and xi is the fraction area given *i*.

2.2. Surface Modification by UVO Treatment

Ultraviolet ozone (UVO) treatment is widely used technology that utilizes ultra violet light and ozone to modify the molecular surface of solids [25]. For most polymers and structured surface, the surface is hydrophobic resulting from nonpolar bonds and is difficult to wet. However, many of printing materials used to coat the surface are hydrophilic. In this regard, they cannot make strong chemical interactions with a hydrophobic surface, and cannot be properly coated. Thus, it is an important issue to develop methods capable of modifying the surface in order to improve its wettability.

Therefore, surface treatments such as oxygen reactive plasma, self-assembled monolayers, and ultraviolet ozone (UVO) treatment are frequently used to modify the surface chemistry and improve wetting characteristics of structured hydrophobic substrate [26-28]. In particular, UVO treatment has advantages of not physically removing material

from the surface and resulting in a much more hydrophilic surface among the others [29].

In UVO treatment for surface modification, oxygen atoms and ozone molecules are continuously created. Most importantly, these highly reactive gases, the atomic oxygen and ozone molecules, are oxidizing agents that may react with surface of substrates to especially form hydroxyl functionalities, which are responsible for the increased wettability of treated surfaces due to property of polarity [30-31]. The number of these radical functionality groups produced during the treatment is dependent on the ozone concentration and UV exposure time [31-32]. While the surface may be greatly modified, the surface of substrate remains physically unchanged, which is the best advantage of utilizing UVO treatment.

3. Experiments

3.1. Preparation of Insulating Banks Made of Photo-curable Polymer

For fabricating the proposed insulating banks, a mixture of poly(dimethylsiloxane) (PDMS) elastomer (Sylgard-184, Dow Corning) and a cross-linking agent (Dow Corning) with a 10:1 weight ratio was first poured onto the pre-patterned master mold in line width and space and then baked at 70℃ for 2 hours. When the cured PDMS was detached from the pre-patterned master mold, it was used as a master mold for the insulating banks through the MIMICs. As illustrated in Fig. 3.1(a) and (b), the pre-patterned PDMS master mold was attached on indium-tin-oxide (ITO) coated glass substrate and an ultraviolet (UV)-curable monomer of NOA74 (Norland) was injected into the channels between a PDMS mold and ITO-coated glass by capillary action. The UV-curable monomer injected into channels was cured under UV light at

the intensity of 100 mW/cm^2 for 60 s and then PDMS master mold was peeled off as shown Fig.3.1(c) and (d). The width of channels (*w*) which is defined as pattern size in Fig.3.1(e) was determined to be 5 and 10 μm.

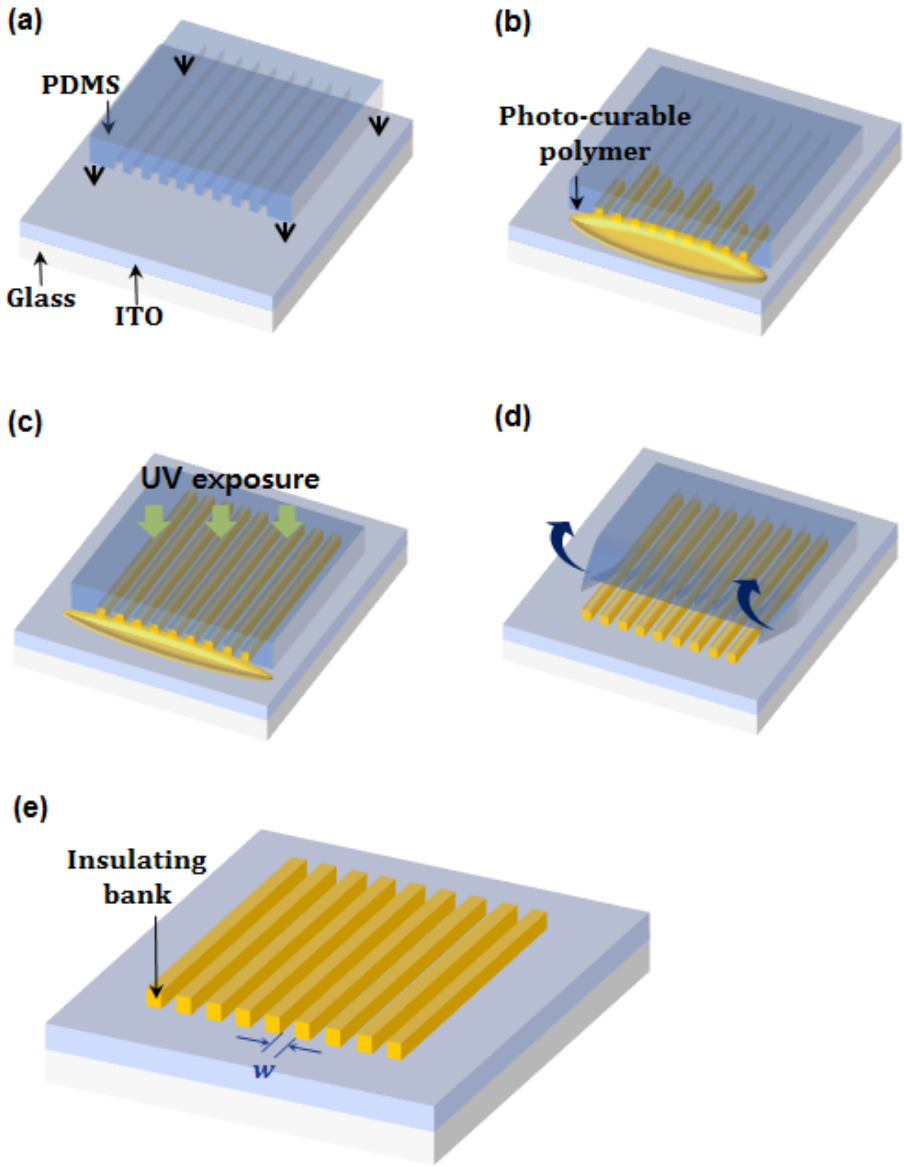

Fig. 3.1 Fabrication of the insulating banks through the MIMICs.

3.2. Fabrication of the patterned S-OLEDs

First, the bank-structured substrate as prepared before was exposed to a UVO flux at the intensity of 28 mW/cm^2 for 30 min in the UVO-chamber (AH-1700, Ahtech LTS Co., Ltd.) under the ambient condition as shown Fig.3.2(a). In this process, ultraviolet light source having two different wavelengths of 184.0 and 253.7 nm is absorbed by atmospheric oxygen, creating oxygen atoms and ozone molecules continuously. Most importantly, these highly reactive gases, the atomic oxygen and ozone molecules, are oxidizing agents that may react with surface of substrates to especially form hydroxyl functionalities, which are responsible for the increased wettability of treated surfaces due to property of polarity. As illustrated in Fig.3.2.(b), the bank-structured substrate was attached by hydroxyl groups after UVO treatment and modified by surface wettability As a result, the intrinsic bank-structured surface, being hydrophobic, became rather hydrophilic due to its polarity.

After that, the S-OLED was fabricated with the bottom-emitting structure which consists of the following layers: ITO/PEDOT:PSS/PDY-

132/LiF/Al, as shown Fig.3.2(c). Poly(3,4-ethylenedioxythiophene) polystyrene sulfonate (PEDOT:PSS) were spin-coated as a hole injection layer at the rate of 2000 rpm for 30 seconds to produce a film thickness of around 50nm. The PEDOT:PSS film was then annealed at 150 ℃ for 10 min. Super Yellow (PDY-132, Merck OLED Materials) with a concentration of 0.6 wt. % in toluene was used to be emission layer and subsequently spin-coated at the rate of 1500 rpm for 60 seconds to produce a thickness of around 60 nm and then annealed at 90 ℃ for 1h. As typical OLED structure, LiF and aluminum was selected as electron injection layer and cathode, respectively. LiF of 0.5 nm was thermally evaporated at the rate of 0.1 Å/s in 3.0 x 10^{-6} Torr. After electron injection layer deposition, aluminum of 100 nm was also evaporated at the rate of 5 Å/s in 3.0 x 10^{-6} Torr.

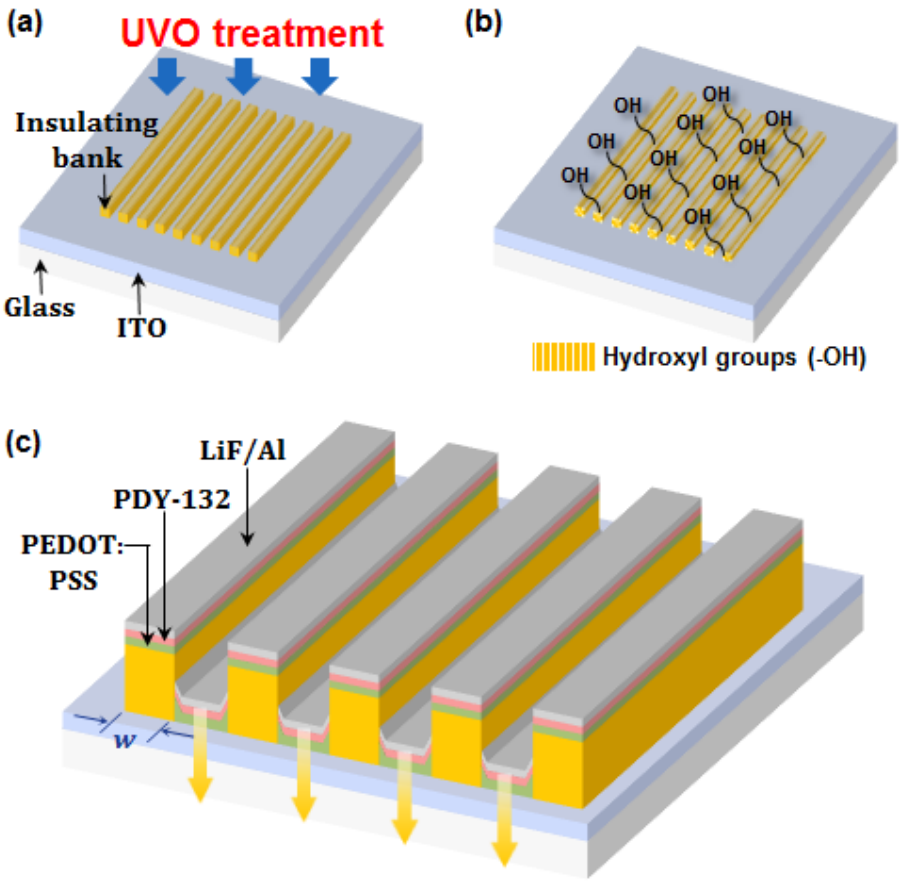

Fig. 3.2 Fabrication of S-OLEDs.

3.3. Measurements of Water Contact Angles on Bank-structured Substrate

One of the crucial surface properties for organic materials in micro substrate is wetting, or hydrophilicity. It is also usually desirable to improve wetting property because of film uniformity of organic solution which is an important factor of device performance. Hydrophilic or hydrophobic properties of a surface wettability are characterized by the static contact angle made between a water droplet and a surface. As illustrated in Fig.3.3, contact angle of water increases with an increase of air pocket formation as patterned-substrate has a higher roughness factor. In this paper, bank-structured substrate fabricated by MIMICs also have a higher roughness factor and expected to be hydrophobic surface due to formation of air pocket. The contact angle of water on the bank-structured substrate was measured as changing line width from 5 μm to 500 μm.

Radical functionality groups like hydroxyl radicals are produced during the UVO treatment. As shown in Fig.3.4, the surface may be modified by

attachment of hydroxyl groups which have polarity after UVO treatment. The contact angle of water on the bank-structured substrate was measured as a function of UVO treatment time.

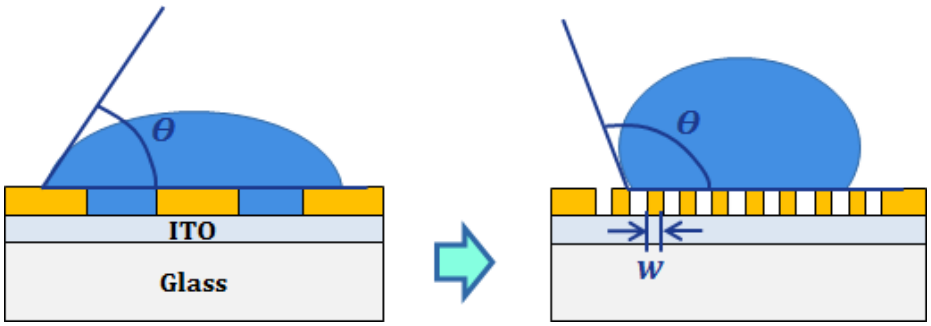

Fig. 3.3 Schematics of water contact angle changes resulting from surface structure density.

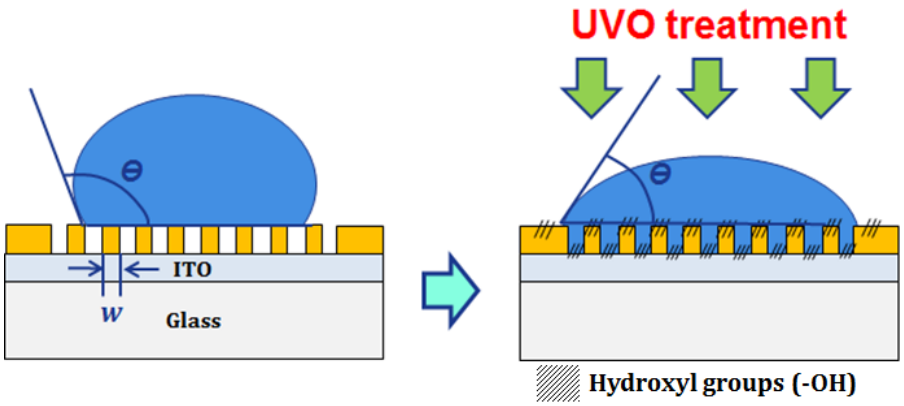

Fig. 3.4 Schematics of transition to hydrophilic surface by surface modification with UVO treatment**.**

4. Results and Discussion

4.1. Contact Angles of Water on the Bank-structured Substrate with Various Line Width

Fig.4.1. shows the scanning electron microscopic (SEM) images of bank-structured substrate prepared by MIMICs. Two types of bank-structured substrate, (a) 5 μm and (b) 10 μm wide, were prepared for fabricating S-OLED device.

We first examined how the density of bank structure for patterning OLED pixels influences the wetting property. Bank structures of 5, 10, 100, 200, 500 μm in line width and space on the ITO-coated glass were prepared by MIMICs. Fig.4.2. shows the photographs of a 5 μL water droplet on the bank-structured substrate as line width (a) 5 μm, (b) 10 μm, (c) 100 μm, (d) 200 μm, (e) 500 μm. It is indicate that the water contact angle increases with increasing in the width density. Fig.4.3. shows the change of water contact

angles for prepared bank structures with corresponding to bank structures of (a) 5, (b) 10, (c) 100, (d) 200, and (e) 500 μm in line width and space, respectively. The contact angle of water on the bank-structured substrate of 500 μm in line width and space was 93.7 deg and it was increased up to 123.3 deg and 117.8 deg with decreasing the width of bank structure to 5 and 10 μm, respectively. It is known as that contact angle increase with an increase of air pocket formation described as Cassie and Baxter's model. In our case, the resolution of OLED pixel, as defined by the line width and space of bank structure, is as small as 5-10 μm. It is indicate that forming thin film of a organic solution on the high-density patterned surface is very difficult without any modification. It is also indicate that forming thin film of a organic solution on the high-density patterned surface is very difficult without any modification.

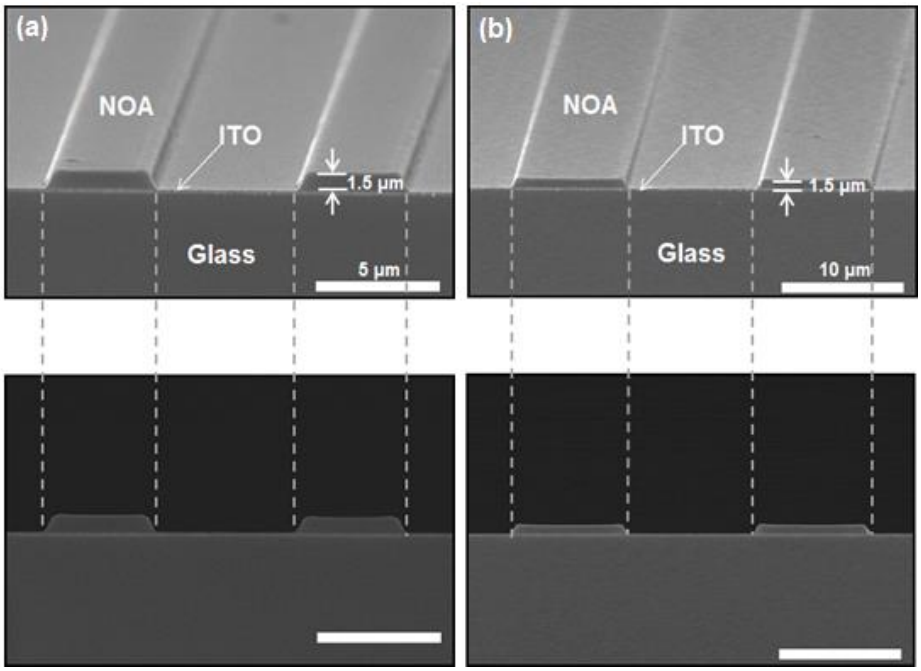

Fig. 4.1 SEM images of insulating banks lines, (a) 5 μm wide and 1.5 μm high, (b) 10 μm wide and 1.5 μm high, produced by MIMICs.

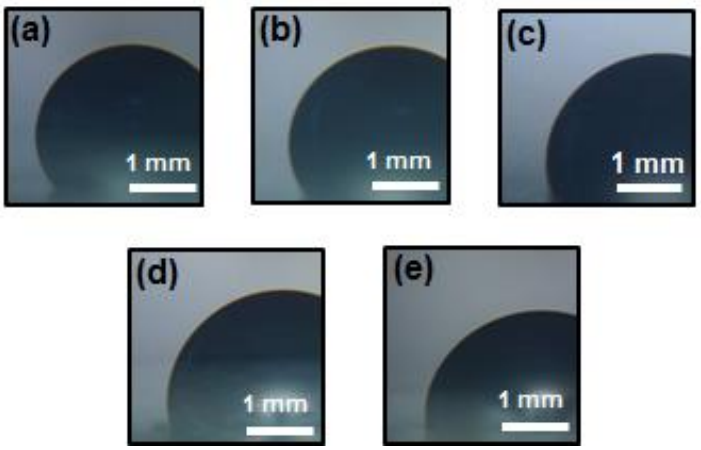

Fig. 4.2 Photographs of a water droplet on the bank-structured substrate as line width (a) 5 μm, (b) 10 μm, (c) 100 μm, (d) 200 μm, (e) 500 μm.

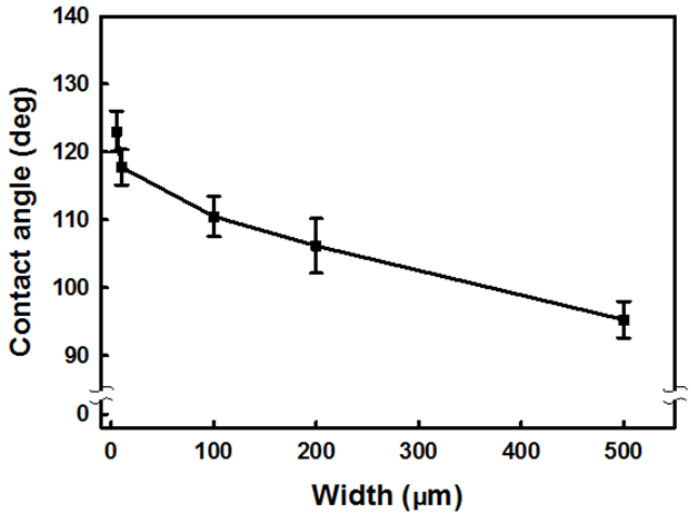

Fig. 4.3 The contact angle of a water droplet on the bank-structured substrate as line width.

4.2. Contact Angles of Water on the Bank-structured Substrate with Increasing UVO treatment Time

We also examined how the UVO treatment for the modification of the bank-structured substrate influences the wetting property of surface. Two types of bank-structured substrate, 5 μm and 10 μm wide, were prepared for fabricating S-OLED device as mentioned before. Fig.4.4 shows the photographs of a 5 μL water droplet on the bank-structured substrate (a) untreated in line width of 5 μm, (b) UVO-treated for 30 min in line width of 5 μm, (c) untreated in line width of 10 μm, (d) UVO-treated for 30 min in line width of 10 μm. Fig. 4.5 also shows the contact angle of water on the bank structure in line width of both 5 and 10 μm was decreased below 20 deg with increasing the duration of the UVO treatment. This means that the bank-structured surface is greatly modified from hydrophobic to hydrophilic by UVO treatment. As a result, the water-based PEDOT:PSS solution is coated directly onto bank-structured substrate modified by UVO treatment uniformly due to attachment of hydroxyl groups which have polarity.

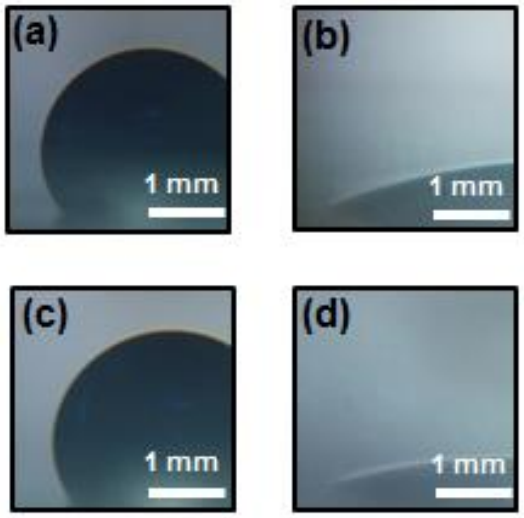

Fig. 4.4 The contact angle of a water droplet on the bank-structured substrate (a) untreated in line width of 5 μm, (b) UVO-treated for 30 min in line width of 5 μm, (c) untreated in line width of 10 μm, (d) UVO-treated for 30 min in line width of 10 μm.

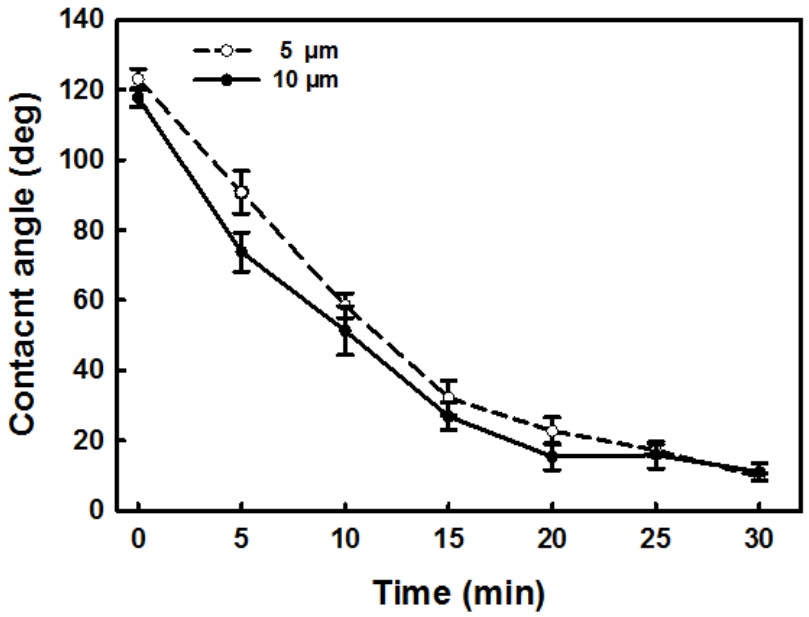

Fig. 4.5 The contact angle of a water droplet on the bank-structured substrate as function of the UVO treatment time. Dashed line corresponds to line width 5 μm, and solid line corresponds to line width 10 μm.

4.3. Microscopic Images of PEDOT:PSS-coated Insulating Banks

As shown in Fig. 4.6 (a) – (c), microscopic images of PEDOT:PSS-coated substrate were observed when the UVO irradiation was not enacted. Fig. 4.6(a) shows the formation of uniform film of PEDOT:PSS on the ITO-coated bare glass substrate. There was no dewetting effect on a organic solution because roughness factor does not exist. Fig. 4.6(b) and (c) show the microscopic images of PEDOT:PSS film on the bank-structured substrate in line width 5 μm and 10 μm, respectively. There were many defects of PEDOT:PSS film on the bank-structured substrate and the formation of non-uniform PEDOT:PSS film was observed. It is due to high roughness factor of microstructure substrate. In contrast, microscopic images of PEDOT:PSS-coated substrate were observed when the surface of substrate was modified by UVO treatment for 30 min as shown in Fig.4.6 (d) – (f). Fig.4.6 (d) shows the formation of uniform film of PEDOT:PSS on the ITO-coated bare glass substrate with UVO treatment for 30 min. There was no difference in uniformity of

PEDOT:PSS compared with untreated ITO-coated glass substrate because roughness factor does not also exist. Fig. 4.6(e) and (f) show the microscopic images of PEDOT:PSS film on the bank-structured substrate with UVO treatment for 20 min in line width 5 μm and 10 μm, respectively. It was confirmed that uniform PEDOT:PSS film was coated on the substrate by surface modification with UVO treatment.

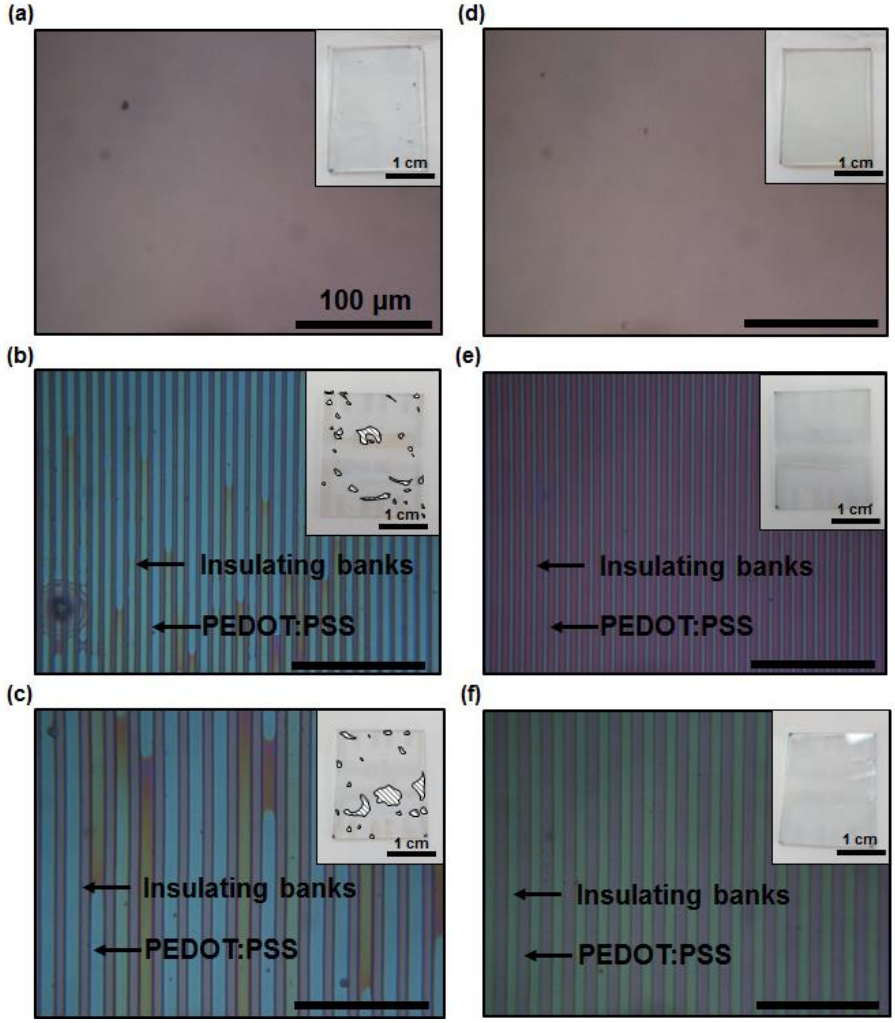

Fig. 4.6 Microscopic images of PEDOT:PSS-coated (a) bare glass, (b) insulating banks (5 μm in line width), and (c) insulating banks (10 μm in line width) without UVO treatment. Microscopic images of PEDOT:PSS-

coated (a) bare class, (b) insulating banks (5 μm in line width), and (c) insulating banks (10 μm in line width) with UVO treatment for 30 min.

4.4. Microscopic Images of the Patterned OLED Device

For the purpose of demonstrating that our patterning approach is practicable, the light-emitting pixels of the device were observed. Fig.4.7. shows the microscopic images of the 5 μm-patterned S-OLEDs at the operating voltages of (a) 4 V, (b) 5 V, (c) 6 V, and (d) 7V. Fig.4.8. corresponds to 10 μm-patterned S-OLEDs. It is clear that the line patterns were well-defined and high fidelity between pixel and black matrix was observed. This indicates that our bank-assisted patterning method is applicable for producing OLED pixels based on solution process. Fig. 4.9 shows light-emitting image of the S-OLED under the applied voltage of 5 V.

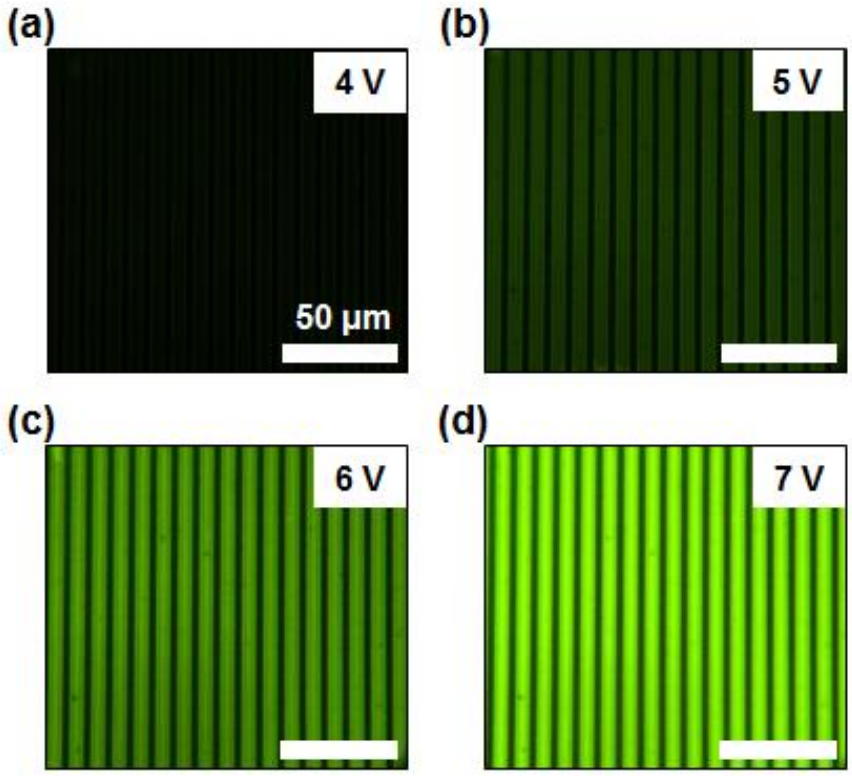

Fig. 4.7 Microscopic images of the 5 μm-patterned S-OLED at the operating voltages of (a) 4 V, (b) 5 V, (c) 6 V, and (d) 7V.

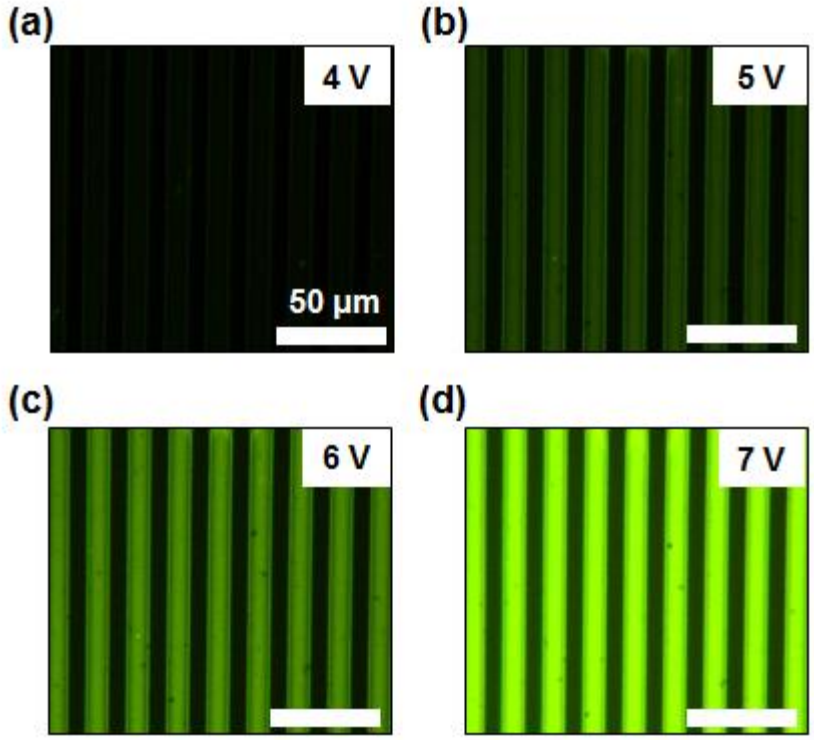

Fig. 4.8 Microscopic images of the 10 μm-patterned S-OLED at the operating voltages of (a) 4 V, (b) 5 V, (c) 6 V, and (d) 7V.

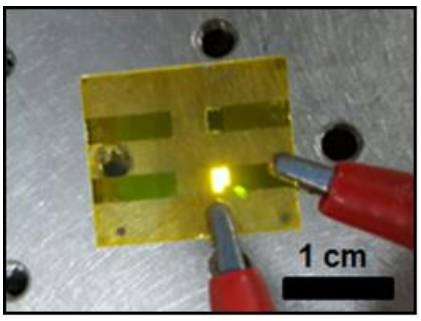

Fig. 4.9 Images of S-OLED device on a glass substrate.

4.5. Electro-optical Characteristics of the Patterned OLED Device

Let us discuss the stability of the light-emitting characteristics of the OLED fabricated by bank-assisted patterning method. It is very important to examine whether the bank structure influences the electroluminescent characteristics of the OLED. The current-voltage-luminance (J-V-L) characteristics were measured by a programmable Keithley model 2400. The J-V-L characteristics of two types of the OLEDs, one of which was non-patterned reference device and the other 5 and 10 μm-patterned device, were shown in Fig. 4.10. Clearly, no appreciable difference in the luminance characteristics between the patterned and non-patterned OLED device was observed as shown in Fig. 4.10. The emission efficiencies of two types of OLEDs are nearly identical to each. It is indicate that our patterning method have no degradation of electro-optical properties in the device performance.

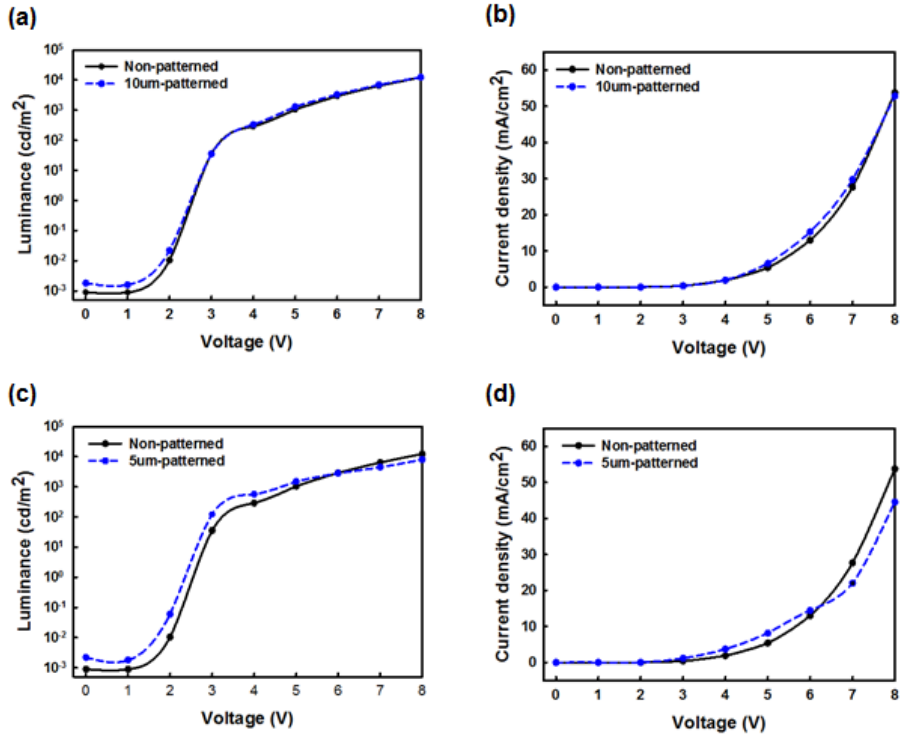

Fig. 4.10 (a), (c) L-V characteristics and (b), (d) J-V characteristics as a function of applied voltages from 0 V to 8 V. Solid line corresponds to non-patterned substrate and dashed line to 5 μm (and 10 μm)-patterned substrate, respectively.

4.6. Electro-optical Characteristics of the Patterned OLED device on the flexible substrate

Solution process has an advantage of applicability of manufacturing OLED on the flexible substrate. Flexibility is one of the features of next generation display because it can promise for ultralight-weight and portable display. As described above, all layers except for cathode in the OLEDs (HIL and EML) are solution-processed. Also, insulating banks made of photo-curable polymer (NOA74) are mechanically soft, allowing the display to be flexible.

The flexible OLED was constructed on the polyethylene naphthalate (PEN) substrate with 5 μm and 10 μm-patterned insulating banks. Insulating banks on the PEN substrate were fabricated with identical process on the glass substrate and OLED materials were stacked with identical conditions.

In order to assure the pixels of S-OLEDs are well-defined, the light-emitting patterns of the flexible device were observed. Fig.4.11 shows the microscopic images of the 5 μm-patterned S-OLED at the operating voltages of (a) 4 V and (b) 7 V, and of the 10 μm-patterned S-OLED at the operating

voltages of (c) 4 V and (d) 7V. It is evident that the pixels of S-OLEDs is well-defined and have uniform features from low to high voltage. In Fig.4.12, (a) working images of at the applied voltage of 5 V and (b) with bending radius of 10 mm are shown.

For the purpose of demonstrating that our patterning approach is applicable for the flexible substrate, the stability of the light-emitting characteristics of the flexible OLED was also measured. Fig. 4.13 shows J-V-L characteristics of two states of the flexible OLEDs, one of which was 5 and 10 μm -patterned of the flat state and the other bending state (10 mm). There was negligible degradation of the device performance after bending patterned OLED as shown in Fig. 4.13. It is indicate that our patterning methods are applicable to flexible display with negligible degradation of electro-optical properties in the device performance. Fig.4.11 (a) shows the characteristics of electroluminance and (b) shows the characteristics of current density as a function of applied voltages from 0 V to 8 V of the 5 μm-patterned device. Fig.4.11 (c) and (d) corresponds to 10 μm-patterned device**.** Solid line

corresponds to flat state and dashed line to bending state with bending radius of 10 mm.

As shown in Fig.4.10 (a) and (c), S-OLED device has a turn on voltage around 1 V to 2 V. For the bending state of flexible S-OLED device, the luminance is largely unchanged compared with flat state. Furthermore, as shown in Fig.4.11 (b) and (d), the characteristics of current density for non-patterned and patterned devices correspond closely. It is indicate that our patterning methods are applicable to flexible display with no degradation of electro-optical properties in the device performance.

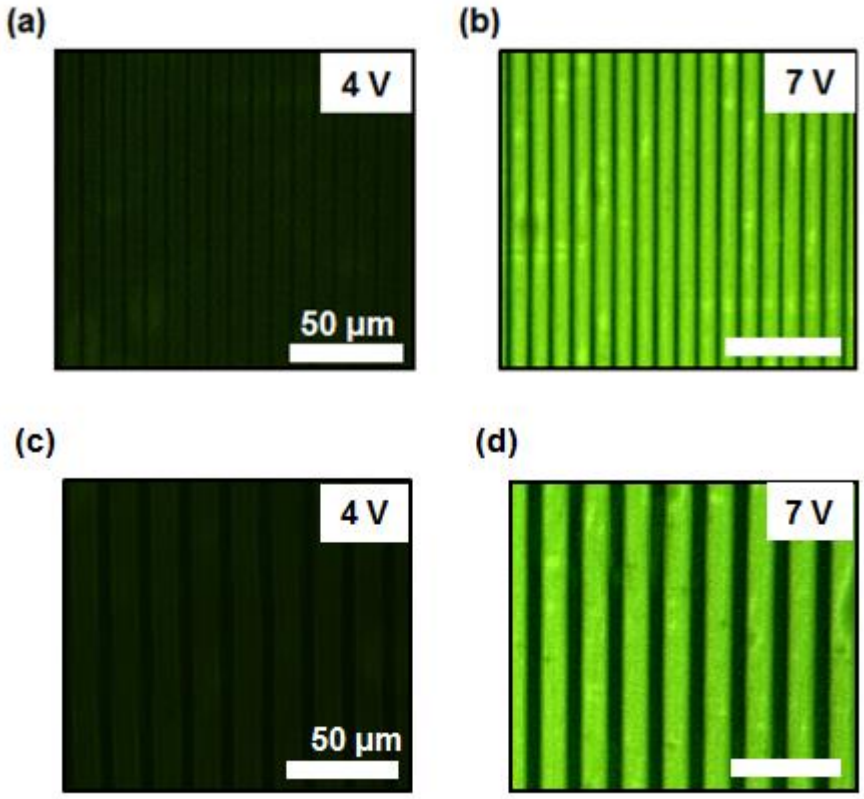

Fig. 4.11 Microscopic images of the S-OLED device (a) 5 μm-patterned at the operating voltage of 4 V and (b) 7 V, and (c) 10 μm-patterned at the operating voltage of 4 V and 7 V.

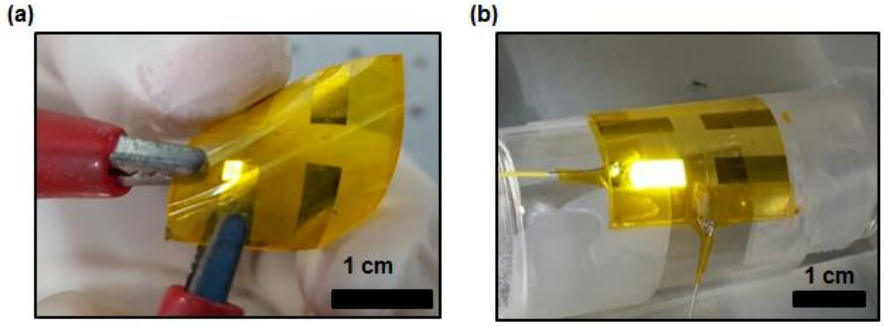

Fig. 4.12 (a) Images of S-OLED device on the flexible substrate (b) with bending radius of 10 mm.

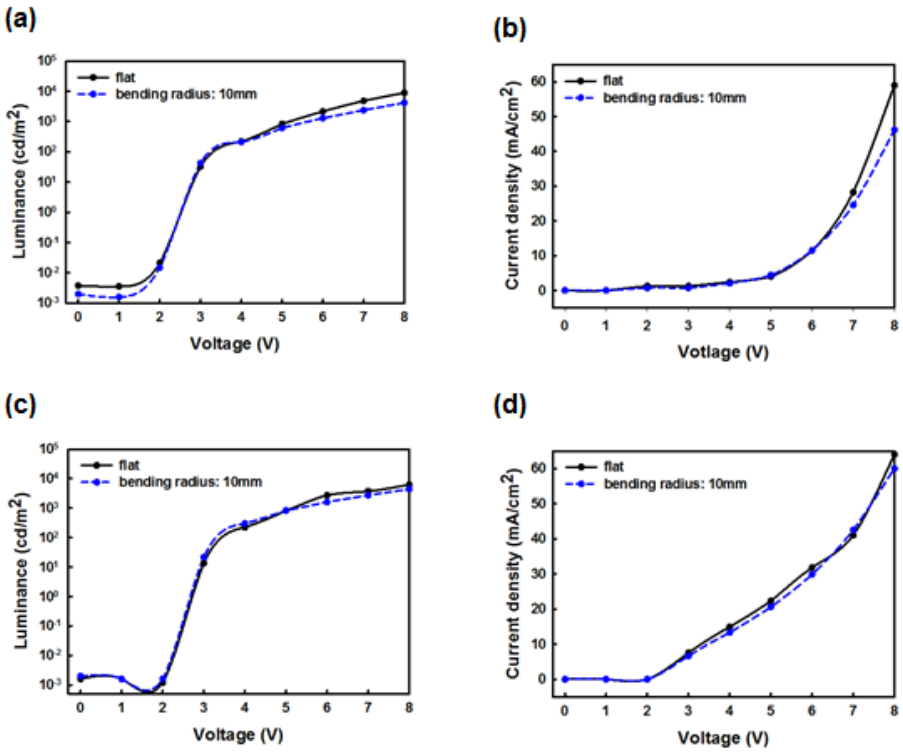

Fig. 4.13 (a), (c) L-V characteristics of the flat state and bending state in 5 and 10 μm-patterned flexible OLEDs, respectively (b), (d) J-V characteristics of the flat state and bending state in 5 and 10 μm-patterned flexible OLEDs, respectively.

5. Conclusion

In this thesis, high-resolution patterning method of solution-processed OLED using surface modified banks by soft lithography was suggested. The surface of bank structure was found to be greatly modified from hydrophobic to hydrophilic with increasing UVO treatment time. Fabricated by softlithographic technique, surface modified bank structure with UVO treatment has improved wetting properties of a organic solution. For the S-OLED device fabricated with the proposed method, the pixels of S-OLED are well-defined and uniform. Also, the L-I-V characteristics of non-patterned and patterned devices correspond closely. Because bank structures made of phot-curable polymer (NOA74) are mechanically soft, it allows the display to be flexible. For the device fabricated on the flexible substrate, the L-I-V characteristics of bending state are also largely unchanged compared with flat state. This wettability-controlled patterning approach will provide a useful platform to construct next generation displays from solutions in the manner of high resolution over large area and low cost. Moreover, the patterned OLED

device has a potential application to microdisplay which requires high density of pixels [33].

Bibliography

[1] C. W. Tang and S. A. VanSlyke, "Organic electroluminescent diodes," Applied Physics Letters, **51**, 913-915 (1987).

[2] M. A. Baldo, D. F. O'Brien, Y. You, A. Shoustikov, S. Sibley, M. E. Thompson, and S. R. Forrest, "Highly efficient phosphorescent emission from organic electroluminescent devices," Nature, **395**, 151-154 (1998).

[3] C. Adachi, M. A. Baldo, M. E. Thompson, and S. R. Forrest, "Nearly 100% internal phosphorescence efficiency in an organic light-emitting device," Journal of Applied Physics, **90**, 5048-5051 (2001)

[4] M. –H. Lu and J. C. Sturm, "Optimization of external coupling and light emission in organic light-emitting devices: modeling and experiment," Journal of Applied Physics, **91**, 595-604 (2002)

[5] M. Agrawal, Y. Sun, S. R. Forrest, and P. Peumans, "Enhanced outcoupling from organic light-emitting diodes using aperiodic dielectric mirrors," Applied physics Letters, **90**, 241112 (2007).

[6] C. C. Wu, C. W. Chen, C. L Lin, and C. J. Yang, "Advanced oragnic light-emitting devices for enhancing display performance," *IEEE/OSA* Journal of Display Technology, **1**, 1226-1229 (2005).

[7] R. S. Cok and A. D. Arnold, "Ambient contrast for OLED disdplay," Digest of Technical Papers –*SID International Symposium*, **38**, 784-787 (2008).

[8] C. Adachi, S. Tokoto, T. Tsutsui, and S. Saito, “Electroluminescence in organic films with three-layer structure,” Japanese Journal of Applied Physics, **27**, 269-271 (1998)..

[9] W. Brutting, *Physics of organic semiconductors*, WILEY-VCH, 2005.

[10] S. Y. Chou, P. R. Krauss, and P. J. Renstrom, “Nanoimprint ithography,” Journal of Vacuum Science & Technology B,” **14**, 4129-4133 (1996).

[11] J.-H. Choi, K.-H. Kim, S.-J. Choi, and H. H. Lee, “Whole device printing for full colour displays with organic light emitting diodes,” Nanotechnology, **17**, 2246 (2006).

[12] E. Kim, Y. Xia, and G. M. Whitesides, “Micromolding in capillaries: application in materials science,” Journal of the American Chemical Society,” **118**, 5722-5731 (1996).

[13] T. Shimoda, K. Morii, S. Seki, and H. Kiguchi, “Inkjet printing of light-emitting polymer displays,” Mrs Bullentin, **28**, 821-827 (2003).

[14] R. Xing, T. Ye, Y. Ding, Z. Ding, D. Ma, and Y. Han, “Thickness uniformity adjustment of inkjet printed light-emitting polymer films by solvent mixture,” Chinese Journal of Chemistry, 31, 1449-1454 (2013).

[15] T. Koyrama, S. Naka, And H. Okada, “Investigation of solution-processed organic light-emitting diode fabrication on patterned line structure using bar-coating method,” Japanese Journal of Applied Physics, 51, 112102, (2012).

[16] S.-H. Jung, J.-J. Kim, and H.-J. Kim, “High performance inkjet printed phosphorescent organic light emitting diodes based on small molecules

commonly used in vacuum processes," Thin Solid Films, **520**, 6954-6958 (2012).

[17] J. Jeong, D. Mascaro, and S. Blair, "Precise pixel patterning of small molecule organic light-emitting devices by spin casting," Organic Electronics, **12**, 2095-2102 (2011).

[18] K. Kim, G. Kim, B. R. Lee, S. Ji, S.-Y. Kim, B. W. An, M. H . Song, and J.-U. Park, Nanoscale, **7**, 13410-13415 (2015).

[19] T. Granlund, T. Nyberg, L. S. Roman, M. Svensson, and O. Inganas, "Patterning of polymer light-emitting didoes with soft lithography," Advanced materials, 12, 269-273 (2000).

[20] F. F. Craig, "The reservoir engineering aspects of waterflooding," Society of Petroleum Engineers, 3, TX (1971).

[21] P. C. Heimenz and R. Rajagopalan, *Principles of colloid and surface chemistry*, Marcel Dekker, New York, 1997.

[22] T. Young, "An essay on the cohesion of fluids," Philosophical Transactions of the Royal Society of London, **95**, 65-87 (1805).

[23] R. N. Wenzel, "Resistance of solid surfaces to wetting by water," Industrial & Engineering Chemistry, **28**, 988-994 (1936).

[24] A. B. D. Cassie, and S. Baxter, "Wettability of porous surfaces," Transactions of the Faraday Society, 40, 546-551 (1944).

[25] N. S. Mcintyre and M. J. Walzak, "New UV/ozone treatment improves adhesiveness of polymer surfaces," **72**, 79-80 (1995)..

[26] T. Bailey, B. J. Choi, M. Colburn, M. Meissl, S, Shaya, J. G. Ekerdt, S. V. Sreenivasan, and C. G. Willson, "Step and flash imprint lithography:

template surface treatment and defect analysis," Journal of Vacuum Science & Technology B, **18**, 3572-3577 (2000).

[27] S. Bhattacharya, A. Datta, J. M. Berg, and S. Gangopadhyay, "Studies on surface wettability of poly(dimethyl) siloxane (PDMS) and glass under oxygen-plasma treatment and correlation with bond strength," Journal of microelectromechanical systems, **14**, 590-597 (2005).

[28] K. Efimenko, W. E. Wallace, and J. Genzer, "Surface modification of sylgard-184 poly(dimethyl siloxane) networks by ultraviolet and ultraviolet/ozone treatment," Journal of colloid and interface sicence, **254**, 306-315 (2002).

[29] M. L. Sham, J. Li, P. C. Ma, J.-K. Kim, "Cleaning an functionalization of polymer surfaces and nanoscale carbon fillers by UV/ozone treatment: a review," Journal of composite materials, **43**, 1537-1564 (2009).

[30] R. P. Singh, N. S. Tomer, and S. V. Bhadraiah, "Photo-oxidation studies on polyurethane coating: effect of additives on yellowing of polyurethane," Polymer degradatoin and stability, **73**, 443-446 (2001).

[31] M. D. R.-Sanchez, M. M. P.-Blas, J. M. M.-Martinez, and M. J. Walzak, "Addition of ozone in the UV radiation treatment of a synthetic styrene-butadiene-styrene (SBS) rubber," **25**, 358-370 (2005).

[32] L. F. Macmanus, M. J. Walzak, and N. S. Mcinture, "Study of ultraviolet light and ozone surface modification of polypropylene, **37**, 2489-2502 (1999).

[33] O. Cakmakci and J. Rolland, “Head-worn display: a review,” Journal of display technology, **2**, 199-216 (2006).

초록

평판 디스플레이 분야에서 용액공정 기반의 유기발광 다이오드는 저비용, 저온, 대면적 공정 적용의 이점으로 주목할 만한 이목을 끌고 있다. 용액공정 다이오드를 제조함에 있어서 간단하고 신뢰성 높은 각각의 화소 패터닝 방법에 대한 연구와 노력들이 이루어져 왔다. 용액 공정 다이오드의 화소를 패터닝하는 기술 중 널리 이용되는 방법 중 하나는 절연둑 구조를 형성하는 방법으로 소자의 성능에 손상을 가하지 않는다는 장점을 지닌다. 그러나 기판위에 고밀도의 절연둑을 형성하는 방법은 본질적으로 용액의 젖음성을 저하시키게 되므로 패턴의 신뢰성뿐만 아니라 해상도 또한 저하시킨다는 단점을 갖는다. 따라서 화소의 고해상도 패턴과 신뢰성을 얻기 위해서는 절연둑 구조를 가지는 기판에 미세한 젖음성 조절이 필수적이다. 본 연구에서는 절연둑 구조를 가지는 기판 위에 자외선 오존 처리를 통한 용액공정 기반의 다이오드의

고해상도 패턴을 형성하는 실행 가능한 방법을 제안한다. 우선, 절연둑은 사전에 패턴된 PDMS와 ITO가 코팅된 유리 기판 사이에 형성된 채널로 광경화성 고분자를 모세관 현상으로 주입되었고 후에 자외선으로 경화시킴으로써 제작되었다. 절연둑 구조를 갖는 기판의 표면 젖음성 조절은 자외선 오존 처리 시간에 따른 표면의 접촉각 측정을 통해 확인되었다. 물의 접촉각의 결과로부터 절연둑 구조의 표면이 소수성에서 친수성으로 매우 크게 변화하였음을 확인할 수 있었다. 5 와 10 마이크로미터의 절연둑 구조가 형성되었고 그에 따른 고해상도의 용액공정 기반 유기발광 다이오드가 제작되었다. 또한, 차세대 디스플레이에 요구되는 특징 중 하나인 유연 기판 위에 동일한 방법으로 용액공정 유기발광 다이오드가 제작되었다. 이러한 젖음성 조절을 통한 접근 방법은 저비용과 대면적 공정의 고해상도 용액공정이라는 장점을 통해 차세대 디스플레이로의 유용한 플랫폼을 제공할 것이다.

주요어: 용액공정 유기발광 다이오드, 접촉각, 소프트 리소그래피, 유기발광다이오드 화소 패턴, 유연기판 디스플레이

학번: 2015-20916